Observation of Carbonyl Fluoride, Ketene, Acetic Acid and Fluorocarbene Produced by an Electric Discharge within a Nozzle by Molecular Beam Fourier Transform Microwave Spectroscopy. A Reaction via a Cycloaddition for Carbonyl Fluoride and Keten?

D. H. Sutter and H. Dreizler

Institut für Physikalische Chemie, Christian-Albrechts-Universität Kiel, Olshausenstraße 40 - 60, D-24098 Kiel

Reprint requests to Prof. H. D.; Fax: +49-431-8801416, E-mail: Dreizler@phc.uni-kiel.de

Z. Naturforsch. 55 a, 695-705 (2000); received June 10, 2000

Prof. Dr. A. Bauder, ETH Zürich, on occasion of his 65th birthday

A molecular beam Fourier transform microwave spectrometer, designed for the study of chemical reactions within electrical discharges, is described in detail. Applications include the production of carbonyl fluoride, ketene, acetic acid, and difluorocarbene. For the production of carbonyl fluoride and ketene with 1,1-difluoroethylene and carbon dioxide as precursor molecules a reaction path via a 2+2 cycloaddition is proposed.

Key words: Reactions and Syntheses in Electric Discharges; Molecular Beam; Product Identification by Fourier Transform Microwave Spectroscopy.

Introduction

For the production of molecular species which are difficult and/or dangerous to synthesize, pyrolysis is a common method in spectroscopy [1]. Application of this method to pulsed molecular beam Fourier transform microwave (MB FTMW) spectroscopy [2] faces several technical difficulties. Harmony et al. [3] report on an instrument with a heated nozzle generating a beam perpendicular to the symmetry axis of the Fabry-Perot cavity. But this arrangement is not optimal in resolution and sensitivity [4], as also mentioned in [3]. An arrangement with coincident molecular beam and resonator axes would improve the sensitivity and resolution. Furthermore, in the setup described in [3] the beam valve is situated inside the vacuum tank, which considerably complicates its adjustment. Quite recently an improved pyrolysis setup with the molecular beam parallel to the resonator axis was tested successfully at our institute by Hansen [5].

As an alternative to pyrolysis we followed work initiated by Grabow et al. [6] and other laboratories [7, 8] and used an electric discharge to initiate reactions within the outlet channel of the nozzle. Within an electric discharge the educt molecules are predomi-

nantly energized by inelastic electron-molecule collisions, i. e. initially the energy is supplied as electronic excitation energy. In other words, the motions of the heavy nuclei are left largely uneffected during the initial excitation process. As a consequence, syntheses of larger molecular species occur much more easily in discharges than in pyrolysis systems.

As applications we report on the production of carbonyl fluoride, F_2CO , ketene, H_2CCO , acetic acid, CH_3COOH , and the free radical fluorocarbene, CF_2 , from different precursors. In a forthcoming publication we will report in detail on fluoroacetylene, FCCH and FCCD, and fuorodiacetylene, FCCCH and FCCCD.

Description of the Spectrometer

The present setup of the MB FTMW spectrometer, which includes many features based on the experience described in [2, 4, 9 - 12], is shown in Figure 1. Basically it contains a Fabry-Perot cavity in a cylindrical tank with the molecular beam coaxial to the symmtry axis of the resonator [4]. The mirrors have a diameter of 60 cm, a curvature of 100 cm and an average distance of 92 cm; adjustable by approximately 16 cm

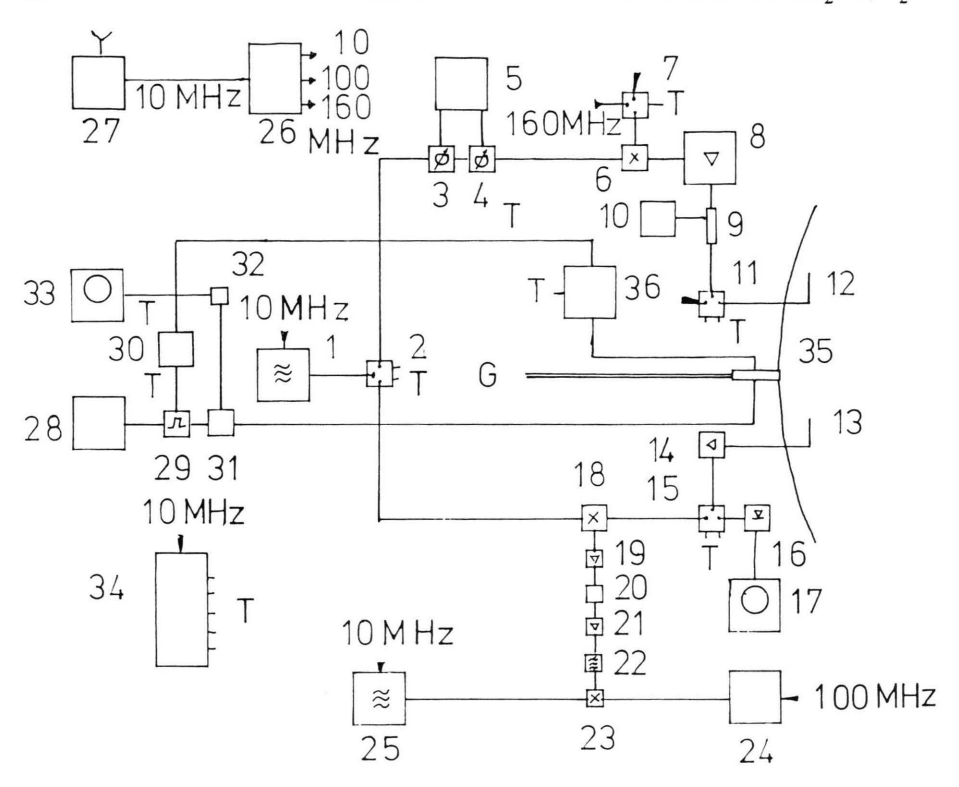
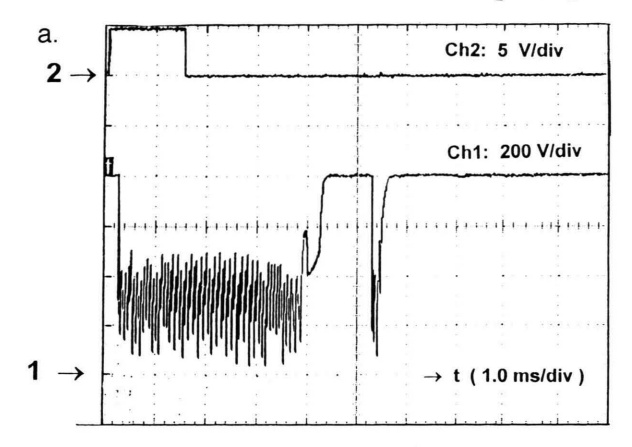


Fig. 1. Setup of the MB FTMW spectrometer for discharge experiments, useable from 3.7 to 22 GHz. 1: MW synthesized sweeper, Hewlett-Packard (HP) 8340 B, 0.1 - 26.5 GHz, 10 dbm, IEEE 488. 2: SPDT-PIN switch, Sierra Microwave Technologies (SMT) 50228, 2 - 26.5 GHz, 60 db isolation, 3.2 db max insertion loss, TTL. 3: Attenuator, HP 84904, DC-26.5 GHz, 11x1 db. 4: Attenuator, HP 84907, DC-26.5 GHz, 7x10 db. 5: Attenuator driver, HP 11713 A, IEEE 488. 6: Single sideband modulator, Miteq SM 0226LC1C, RF/IF 0/10 db, conversion loss 12 db typ. 7: SPDT-PIN switch, Mini Circuits ZYSWA-2-50DR, DC-500 MHz, isolation 40 db, TTL. 8: MW-amplifier, HP 8348 A, 2 - 26.5 GHz, gain 25 - 23 db, noise figure (NF) 10 - 13 db. 9: Directional coupler, HP 87301 D, -40 GHz, coupling 13 db. 10: Power meter, HP 435B or HP 437 B with sensor HP 8485 A, -26.5 GHz, optional. 11: SPDT-PIN switch, SMT 50254 with termination, see 2. 12: L-shaped antenna for polarisation, adjustable in orientation from outside. 13: L-shaped antenna for detection, adjustable in orientation from outside. 14: Low noise amplifier, Miteq JS4001018-23-5P, 0.1 - 18 GHz, NF 2.3 db, gain 29 db. 15: SPDT-PIN switch, SMT 50254, see 2. 16: MW-diode, HP 8474D, 0.1 - 40 GHz. 17: Oszilloscope, Tektronix 2235. 18: Image rejection mixer, Miteq IR00226, 2 - 26 GHz, Lo 10 dbm, image rejection 20 db, conversion loss 10 db. 19: IF-amplifier, Trontech L160 B, 160 MHz, gain 50 db, NF < 1.4 db. 20: Adjustable attenuator, Weinschel 10x1 db, 7x10 db. 21: If-amplifier, Trontech L160 A, 160 MHz, gain 40 db, NF < 1.4 db. 22: BP-filter, Reactel 4B2-160-2, 160 MHz, bandwidth 2 MHz. 23: IF-mixer, Mini Circuits ZAD1, LO/RF 0.5 - 500 MHz. IF DC-500 MHz. 24: ADC, Spectrum PAD82, 10 ns stepwidth min and PC with program by J.-U. Grabow. 25: Synthesizer, PTS 160, 0.1 - 160 MHz, 13 dbm. 26: Frequency multiplier, home made. 27: Normal frequency receiver, Rhode&Schwarz XKE2+XSD2 and quartz oscillator. 28: Power supply, Fluke 315 B, 0 - 3000 V, 30 mA. 29: High voltage switch, Behlke HTS31-03-GSM. 30: Pulse generator HP 8005 A. 31: Limiting resistor, 29 k ohm. 32: HV-probe, Tektronix P5100. 33: Oscilloscope, Tektronix TDS 320. 34: TTL pulse driver, home made, U. Andresen. 35: Beam nozzle, General Valve series 9 with discharge electrodes, home made. 36: Nozzle driver, General Valve Iota I. T: TTL output/input. G: Gas input.

for tuning to the microwave frequency used for polarisation. The beam nozzle 35 (see Fig. 1) and the input and output antennas 12 and 13, mounted in the stationary mirror, are accessible and adjustable for their performance from outside the vacuum tank. Also the mechanical settings of the valve and the orientation of

the antennas can be optimized by observation of the molecular signal in real time, which is a useful feature. Windows allow an easy exchange of the L-type antennas and the direct observation of the discharge. One antenna is used for polarisation of the molecular ensemble, one antenna receives the molecular signal.



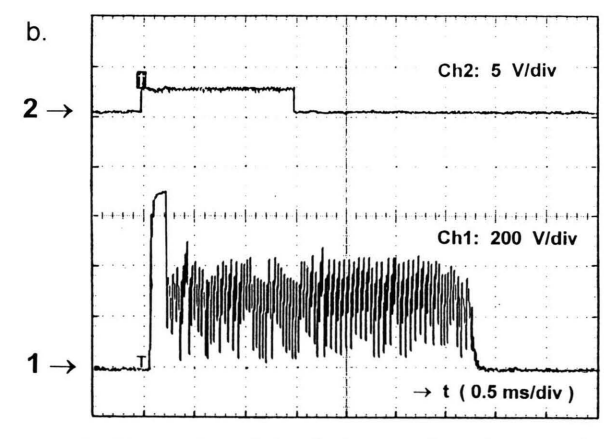


Fig. 2. Observation of the discharge voltage between the electrodes within the the nozzle by oscilloscope **33** of Figure 1.

a) Trace 2: TTL signal of 1.5 ms length from **36** for activating the beam valve **35**. Trace 1: Discharge voltage of 800 V permanently applied dropping approximately to 0 V caused by the discharge through the pulsed gas stream for 4 ms in a periodic manner, followed by an unintended reopening of the valve and additional ignition of 0.2 ms length.

b) Trace 2: TTL signal of 1.5 ms length of 36. Trace 1: Discharge adjusted with HV-switch 29 of approximately 3 ms length following a peak, indicating 700 V applied discharge voltage, with some delay with respect to the signal of trace 2.

The latter antenna is directly connected to a low noise broad band amplifier.

For polarisation the MW of frequency ν from 1 is guided to the antenna 12 by the single pole double throw (SPDT) switch 2, adjusted in power 3 - 5, converted to ν + 160 MHz by the single sideband modulator 6, amplified by 8 and pulse modulated by 7 and 11.

The directional coupler 9 and power meter 10 are used for power monitoring.

In the detection phase, the signal of the molecular ensemble is received by the separate antenna 13, low noise amplified by 14 and guided to the image rejection mixer 18 by the SPDT switch 15. It is heterodvned down into a frequency band around 160 MHz with the local power from 1, directed to 18 by 2. The downconverted signal is amplified by 19 and 21. The adjustable attenuator 20 prevents resonant feed back oscillations and possible power saturation. By the mixer 23 and the adjustable radiofrequency local oscillator 25 the signal is again downconverted to frequencies close to 2.5 MHz and A/D converted with a transient recorder incorporated in 24. Further signal processing by fast Fourier transformation is performed by a personal computer 24, which is also used to control the settings of the spectrometer. The program was written by J.-U. Grabow.

For adjustment of the cavity resonance to the microwave frequency, the diode 16 is used with an appropriate setting of the switches 2, 7, 11 and 15.

The essential changes in comparison to former setups are the use of two antennas and the direct connection of the low noise amplifier 14 to the antenna 13. This lowers the noise figure of the spectrometer at least by the insertion loss (attenuation approximately 3 db) of the usually used switch to protect the detection system. See for example part 2c in Fig. 1 of [2].

The discharge nozzle first described in [6] was replaced by a construction given in Fig. 8 of [12], but modified in details. Part of the TeflonTM spacers have been replaced by MarcorTM ceramic spacers with a different position of the O-rings. The material was obtained from E + P Fiber Optic, CH-8957 Spreitenbach. These MarcorTM spacers withstand longer to the discharge produced by 800 to 1500 V between the ring electrodes. They show less carbonic deposites and they could be cleaned more easily. Application of a positive voltage to the upstream electrode with the downstream electrode on ground proved to be more efficient in our experiments. Nevertheless, the discharge nozzle is still the weakest part of the spectrometer, as the period of good performance varied from six hours to 60 hours. After such a period the valve has to be dismounted, cleaned and readjusted. The tank has to be evacuated again. Furthermore the beam valve 35 tends to reopen for a short period after the intended opening of 1 to 2 ms inducing a discharge of a length of 3 ms by self ignition and an irregular discharge of a length of approximately 0.2 ms as shown in Figure 2a). In Fig. 2b) a carefully adjusted discharge is shown. Usually the discharge can be observed as a weak light cone in front of the nozzle mouth. But sometimes a heavy arcing could be observed, presumably associated with an irregular opening of the valve. This may be a lethal danger for the microwave parts connected to the antennas, which are positioned only 2 cm away.

An unwanted irregular discharge can be suppressed if a high voltage switch 29 is used to apply the high voltage from 28 to the electrodes with its duration and its delay with respect to the trigger pulse adjustable by the pulse generator 30. With this arrangement the most effective production region within the molecular beam can also be chosen.

Measurements

Primarily the aim of our measurements was to identify reaction products by their rotational spectra. As examples we have chosen several halogenated hydrocarbons as precursors. These compounds are of interest also as anthropogenic atmospheric trace gases. Since the experimental precision of the frequency determinations is high, approximately 1:10⁷ and better, generally one transition is sufficient for identification.

a) Carbonylfluoride and Ketene, from 1,1-difluoroethylene and Carbon Dioxide; Vibronic Ground State Spectra

As precursor molecules for the production of carbonyl fluoride we have used 1,1-difluoroethylene, H₂CCF₂, and carbon dioxide, CO₂, supplied by Fa. Aldrich, Steinheim, and Fa. Messer Griesheim, Krefeld, respectively. Mixtures of 1% H₂CCF₂ and 1 to 3% of CO₂ in argon, which serves as an inert carrier gas, were introduced into the beam nozzle with 700 to 1500 V applied to the electrodes. Typical backing pressures ranged between 1 and 1.5 bar. Upon discharge through this gas mixture a rotational transition of fluoroacetylene, FCCH, can be observed already with one-cycle experiments. We therefore believe that the predominant reaction pathway for H₂CCF₂ starts with the monomolecular elimination reaction

$$H_2CCF_2 \rightarrow FCCH + HF.$$
 (1)

We note that this reaction has been studied recently also by Lin and Lee [13] by use of laser photolysis to energize the educt molecules and step-scan timeresolved Fourier transform infrared emission spectroscopy for detection. These authors have carefully studied the time evolution of the vibrational populations of the second reaction product, HF. We will treat this main reaction pathway as part of a separate publication [14].

As noted above, direct fragmentation products, such as FCCH in the present case, can be detected already in one-cycle experiments with our experimental setup. The observation of the products of bimolecular reactions requires the accumulation of considerably more free induction decay (FID) signals for reasonable signal to noise ratios. This reflects the fact that molecule-molecule collisions are comparatively rare within the sparsely seeded beam. Molecules mostly collide with the abundant carrier gas atoms. Further downstream, collisions even practically cease within the supersonic beam. This effectively suppresses reactions which require two separate subunits to collide already few µs after the particles have been exposed to the discharge.

In the following we report on a second reaction pathway. It leads to the production of carbonyl fluoride and ketene. Both product molecules were detected by their $J_{K_aK_c} = 1_{01} \rightarrow 0_{00}$ a-type rotational transitions. For F₂CO additional five transitions could be observed for even better identification. Quite typical for the products created in bimolecular collisions within a sparsely seeded beam, larger numbers of FIDs must be accumulated for detection. In the present study we had to add up typically 128 to 4096 FIDs in the case of F₂CO. In the case of H₂CCO the number was even higher, i. e. typically 4096 to 12596. As a consequence, the experimental conditions like polarization power, microwave pulse length, and delays could be adjusted only roughly, because of the long averaging times. In view of the limited pumping power of our present vacuum system we also had to reduce the pulse repetition rate to 2 Hz for good performance.

Our measured rotational transition frequencies, six for F_2CO and one for H_2CCO , are listed in Table 1. The frequencies were obtained by a Levenberg-Marquardt fit of the frequencies, amplitudes, phases, relaxation time and beam velocity to the time domain signal [15, 16]. The program of [16] was used. With six lines for F_2CO [17], three of them with characteristic spin-rotation hyperfine structure [18, 19], there is no doubt that the substance was produced. For all lines it was also checked that no signal appears without a discharge.

Table 1. Measured transitions refined by a fit of the time domain signal [15, 16] of carbonyl fluoride, F_2CO , ketene, $H_2C=C=O$, acetic acid, CH_3COOH , and difluorocarbene, CF_2 . ν mean value of fitted frequencies (for F_2CO center frequency of multiplets, for CH_3COOH peak of the unresolved multiplets) and deviation in brackets of several measurements, C number of averaging cycles, ν_{lit} literature value of measurement.

ture varu	ie of measurement.			
$J_{K_aK_c}$ -	$J'_{K_{a'}K_{c'}}$ ν [MHz]	C	ν_{lit} [MHz]	
Transition	ns of F ₂ CO:			
$\begin{array}{c} 1_{11} - 1_{10} \\ 2_{21} - 2_{20} \\ 3_{31} - 3_{30} \\ 1_{01} - 0_{00} \\ 2_{11} - 2_{12} \\ 3_{21} - 3_{22} \end{array}$	5872.1208(12) 5812.0299(4) 5722.842(2) 17633.9301(1) 17616.2372(1) 17525.4733(1)	512 to 4096 128 to 2048 512 to 1024 128 to 1024 1024 2048	5872.180 5812.160 5722.840 17633.941 17616.239 17525.463	[17] [17] [17] [17] [17]
	ns of H ₂ C=C=O:			
1_{01} - 0_{00}	20209.2105(8)* 20209.21105(10)**	4096 to 12600 16 to 1024	20209.20	[24]
$ \begin{array}{c} 1_{01} - 0_{00} \\ v_9 = 1 **** \end{array} $	20266.8787(2)	512	20266.86 20266.865	[24] [25]
Transition	ns of CH ₃ COOH:			
1 ₁₁ -0 ₀₀ 2 ₁₁ -2 ₀₂	A 16741.4938 E 16418.4492 A 12989.9093 E 13025.2735	512 1024 512 512	16741.55 16418.55 12989.92 13025.28	[23] [23] [23] [23]
Transition	n of CF ₂ :			
4 ₀₄ -3 ₁₃	21500.1683(1)	1024, 22675	21500.1696 21500.1	[26] [28]

^{*} precursor H₂CCF₂ + CO₂, ** precursor (CH₃CO)₂O, *** for designation of the vibrational states see [25].

We believe that F₂CO and H₂CCO are created in a two step reaction. First a cycloaddition of appropriately activated precursor molecules leads to an intermediate, strained four-ring, nascent in a highly excited state, which readily fragmentates again back into the precursor molecules or, as an alternative, into our target molecules, carbonylfluoride and ketene:

Such cycloadditions and cycloreversions are a common concept in reaction kinetics since long [20].

In principle a second pathway, which also involves a cycloaddition as intermediate step, should be considered too:

$$F_{2}C=CH_{2} \qquad F_{2}C-CH_{2} \qquad F \qquad F \qquad H \qquad H$$

$$+ \qquad \Rightarrow \qquad | \qquad | \qquad \Rightarrow \qquad C \qquad + \qquad C$$

$$O=C=O \qquad O=C-O \qquad C \qquad O$$

$$O \qquad O \qquad O \qquad O$$

But in view of the partial atomic charge distribution within the reaction partners, it appears to be unlikely that the latter sequence of reactions should occur frequently. In the final stage of approach, immediately prior to cyclization, Coulomb interaction will tend to force the two subunits into the relative arrangement which leads to carbonylfluoride and ketene as the final products. We note, however, that a careful search for formaldehyde, difluoroketene and other species has not yet been carried out by us.

In Figs. 3 and 4 a,b) we present registrations of the $1_{0.1} \rightarrow 0_{0.0}$ transitions of F₂CO and H₂CCO, respectively. The Doppler splitting is only slightly increased with respect to the situation in the absence of a discharge. This demonstrates that the translational (and rotational) temperature of the gas is raised only very little by application of a discharge. For an estimate of this rise in temperature we assume an adiabatic expansion in which the free enthalpy contents of the carrier gas, here argon, is completely transformed into directed translational energy. Within this assumption the relation $mv^2/2 = 5kT/2$ should hold with m =mass of a carrier gas atom, here argon, k = Boltzmann's constant, T = temperature of the gas in the storage vessel in front of the nozzle and v = final velocity of the atoms (and molecules) within the beam. The latter is reached already within the first centimeters downstream of the mouth of the nozzle, such that the bulk of the molecules travels at practically the same speed through the cavity. For T = 300 K(room temperature), as was used in our experiments, this leads to v = 558 m/s, just as was observed for the parent molecules in the absence of a discharge. From the slightly larger Doppler splittings observed with a discharge, beam velocities between 570 and 610 m/s are deduced. The exact value depends on the discharge voltage. These beam velocities translate into temperatures between 310 and 360 K at the outlet of the nozzle. This agrees with our assumption that the exitation energy is predominantly supplied by inelastic electron-atom and electron-molecule collisions, i.e. as electronic excitation energy, quite in contrast to the situation in a heated nozzle [3], where the energy is primarily supplied to the nuclei as translational energy, and in the case of molecules also as rotational and vibrational energy of the nuclear

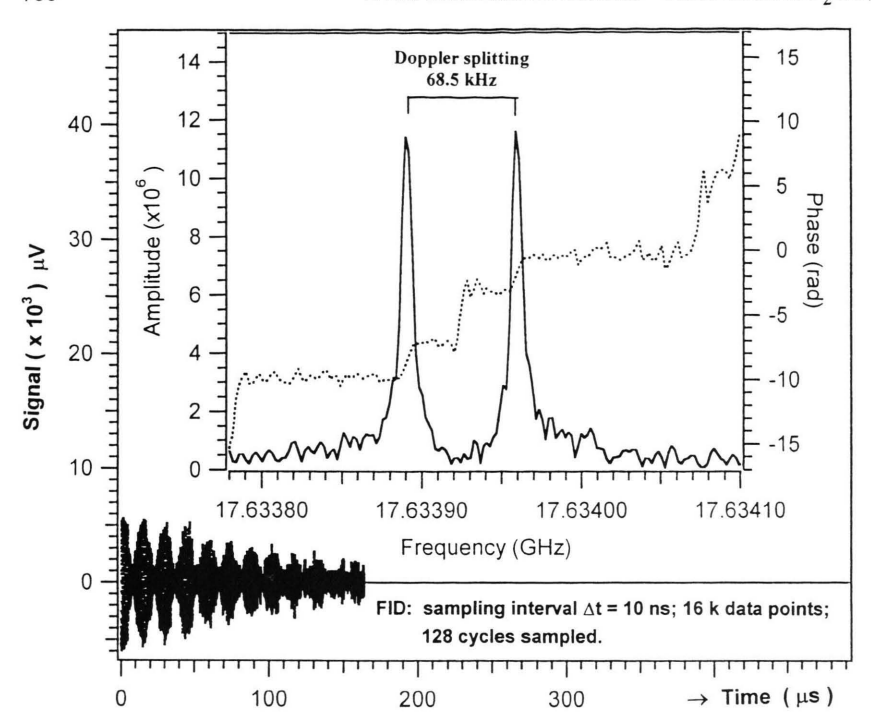


Fig. 3. Time domain signal of the $J_{K_aK_c} = 1_{01} - 0_{00}$ transition of F₂CO produced by the bimolecular reaction H₂CCF₂ + CO₂ = F₂CO + H₂CCO. 17633.92 MHz polarisation frequency. *Insert:* Amplitude spectrum showing the Doppler doublet and phase spectrum.

frame. This difference in the excitation mechanism quite naturally also leads to different types of reactions. While cracking into smaller subunits is typical for pyrolysis systems, also larger molecules such as for instance long chains may assemble in the comparatively "cold" gas mixture immediately downstream of the discharge region, if the excitation energy is supplied by a discharge [21].

Since for ketene our observed transition frequency did not perfectly match the value reported in the literature, we have also tried additional production schemes.

First we tried to mix ketene with argon in a stainless steel cylinder and to observe its free induction decay signals following microwave pulse excitation directly, i. e. with the discharge turned off. The ketene had been prepared separately at our institute by J. Gripp, who used the well known method of pyrolysis [22] with acetic anhydride supplied by Fa. Aldrich, Steinheim, as precursor. This attempt failed, presumably because ketene readily polymerizes at room temperature. This would leave only few ketene monomers in the gas mixture.

Second we supplied the same precursor, i. e. acetic anhydride, in a stainless steel vessel 20 cm upstream of the nozzle of our discharge system. A stream of argon at 1.1 bar was guided through this vessel and

the resulting gas mixture was fed to the nozzle. With the discharge turned on, ketene was produced very effectively. With only 16 free induction decay signals accumulated (16 cycles), a pleasing signal to noise ratio of 76:1 was obtained in the Fourier transform amplitude spectrum. As mentioned already, such strong signals are typical for products which are produced in a monomolecular reaction.

Our measured frequency for the 1_{01} - 0_{00} transition is added in Table 1. It agrees within 500 Hz with the frequency observed in the reaction products of H_2CCF_2 with CO_2 , an agreement which is quite reasonable in view of the comparatively noisy spectra observed in the latter production scheme. The strong signal given in Fig. 5 suggests that ketene is produced in the elimination reaction

$$(CH_3CO)_2O \rightarrow H_2CCO + H_3COOH.$$
 (4)

We therefore also searched for the second fragmentation product, acetic acid, CH₃COOH, which was readily identified by four transitions given in [23].

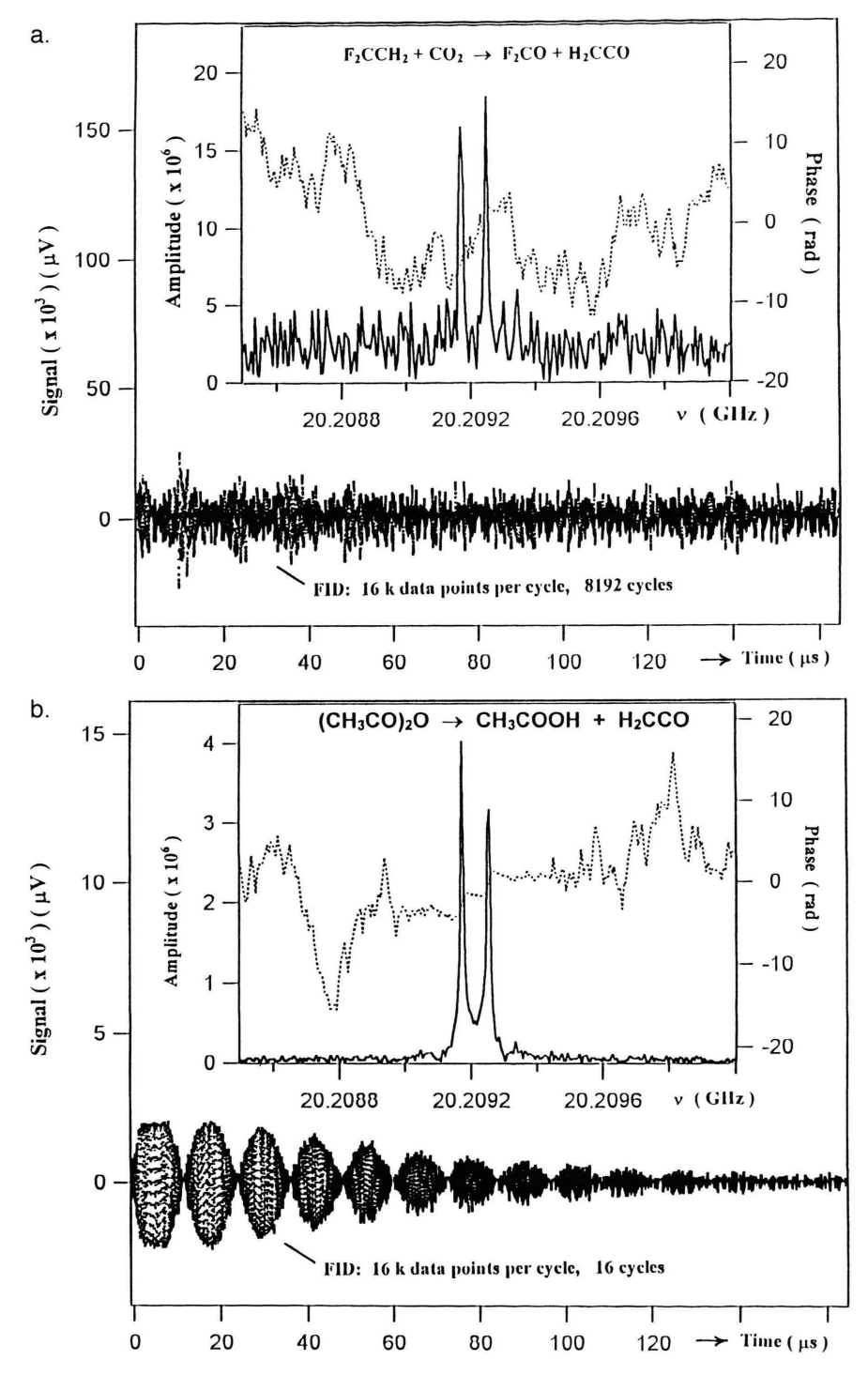


Fig. 4. a) Time domain signal of the 1_{01} - 0 $_{00}$ transition of H_2CCO produced by the bimolecular reaction. 20209.21 MHz polarisation frequency, 78.9 kHz Doppler splitting, 1500 V discharge voltage. *Insert:* Amplitude and phase spectrum. b) Time domain signal of the same transition of H_2CCO produced in the monomolecular reaction 4. Same conditions as in Fig. 4a), but only 16 cycles and 1400 V discharge voltage. 82.1 kHz Doppler splitting. *Insert:* Amplitude and phase spectrum with a much better S/N ratio indicating a more effective production of H_2CCO , resulting in an initial saturation of the detection system.

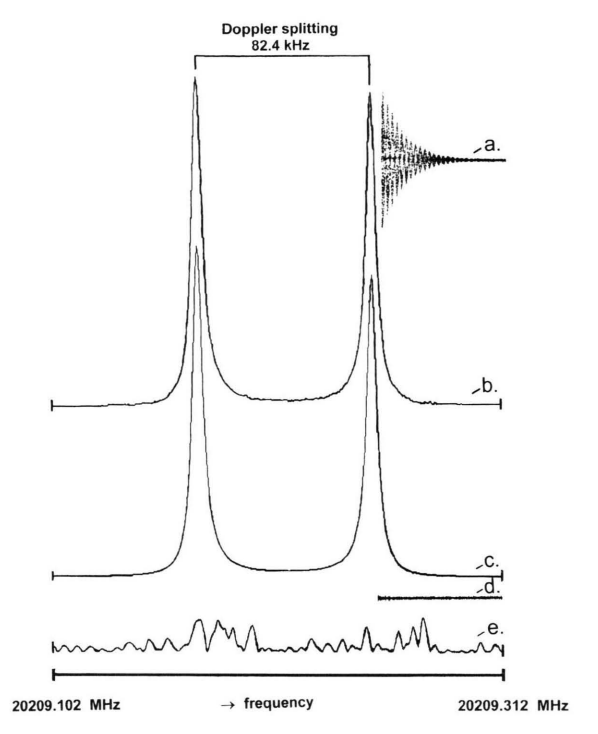


Fig. 5. Evaluation of a recording of the 1_{01} - 0_{00} transition of H_2CCO produced from $(H_3CCO)_2O$. 40 ns step width, 16 k data points, 20209.21 MHz polarisation frequency, 512 cycles. a) Time domain signal; b) Amplitude spectrum; c) Amplitude spectrum resulting from a fit to the time domain signal a (see text); d) Residuum time domain signal; e) Fourier transform of the residual FID (noise).

They too are presented in Table 1. In Fig. 6a) we present the Fourier transform amplitude spectrum of the $1_{11} \rightarrow 0_{00}$ rotational transition in the A-state of the methyl top internal rotation of acetic acid as an example. Note that its linewidth is comparatively large due to the incompletely resolved additional hyperfine structure, which is caused by proton spin-spin and spin-rotation interaction. In Fig. 6b) we tried to reveal the fine structure more clearly.

Excited vibrational states of ketene

From the reaction scheme (4) one expects a highly non thermal nascent vibrational distribution. Especially higher states of the bending vibrations [24], primarily of the ν_9 -mode [24], are expected to show populations in excess with respect to their thermal population values. Since in a supersonic expansion vibrational relaxation is much less effective than rotational relaxation, we expected to find sizable vi-

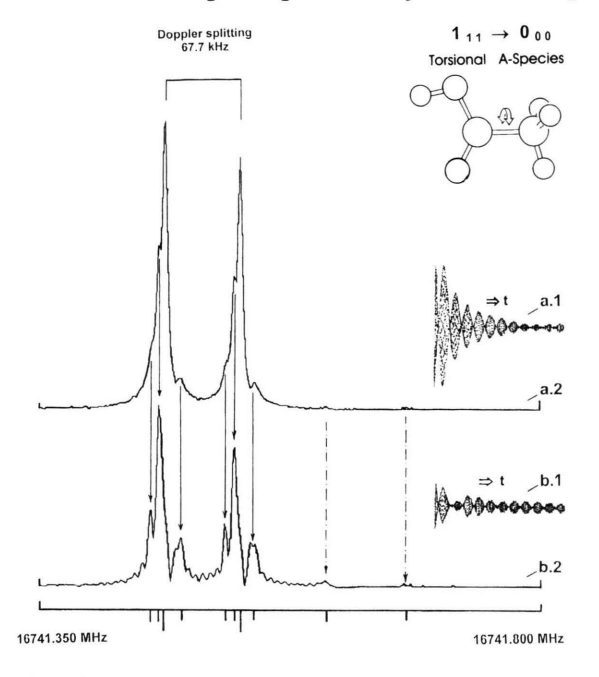


Fig. 6. a.1) Time domain signal of the 1₁₁ - 0 ₀₀, torsion A species, transition of CH₃COOH, produced with (CH₃CO)₂O. 20 ns step width, 16 k data points, 16741.55 MHz, polarisation frequency, 512 cycles. a.2) Amplitude spectrum calculated with FID of a.1), showing an indication of a spin rotation fine structure, which was not analysed for the four H atoms. 6b.1) Time domain signal after elimination of the strongest component. b.2) Amplitude spectrum caculated with FID of b.1) showing features of the spin-rotation coupling more clearly. The features of b.2) are correlated to those of a.2). The cutoff of the FID b.1) causes wiggles in the FT-spectrum.

brational rest-populations quasi frozen in the almost collisionless environment of the expanding beam.

With the rotational constants and centrifugal distortion constants of three vibrational states of ketene, well known from the work of Hinze *et al.* [25], we could predict the frequencies of the $J_{K_aK_c}$ = $1_{0.1}$ - $0_{0.0}$ transition in the states ν_9 (439.0 cm⁻¹), ν_6 (528.4 cm⁻¹), and ν_5 (587.3 cm⁻¹) for a search.

In Table 1 our measured frequency for the transition in the first excited state of the ν_9 -vibration is added. It agrees reasonably well with values cited in the quoted literature. To our surprise we could not observe lines reliably for the ν_6 - and ν_5 -states. The quotient of the signal to noise ratios of the $1_{0\,1}$ - $0_{0\,0}$ transitions in the ground state and in the first excited state of the ν_9 -vibration was roughly 4. The measurements were performed with the same number of cycles (512) and under nearly the same polarization conditions.

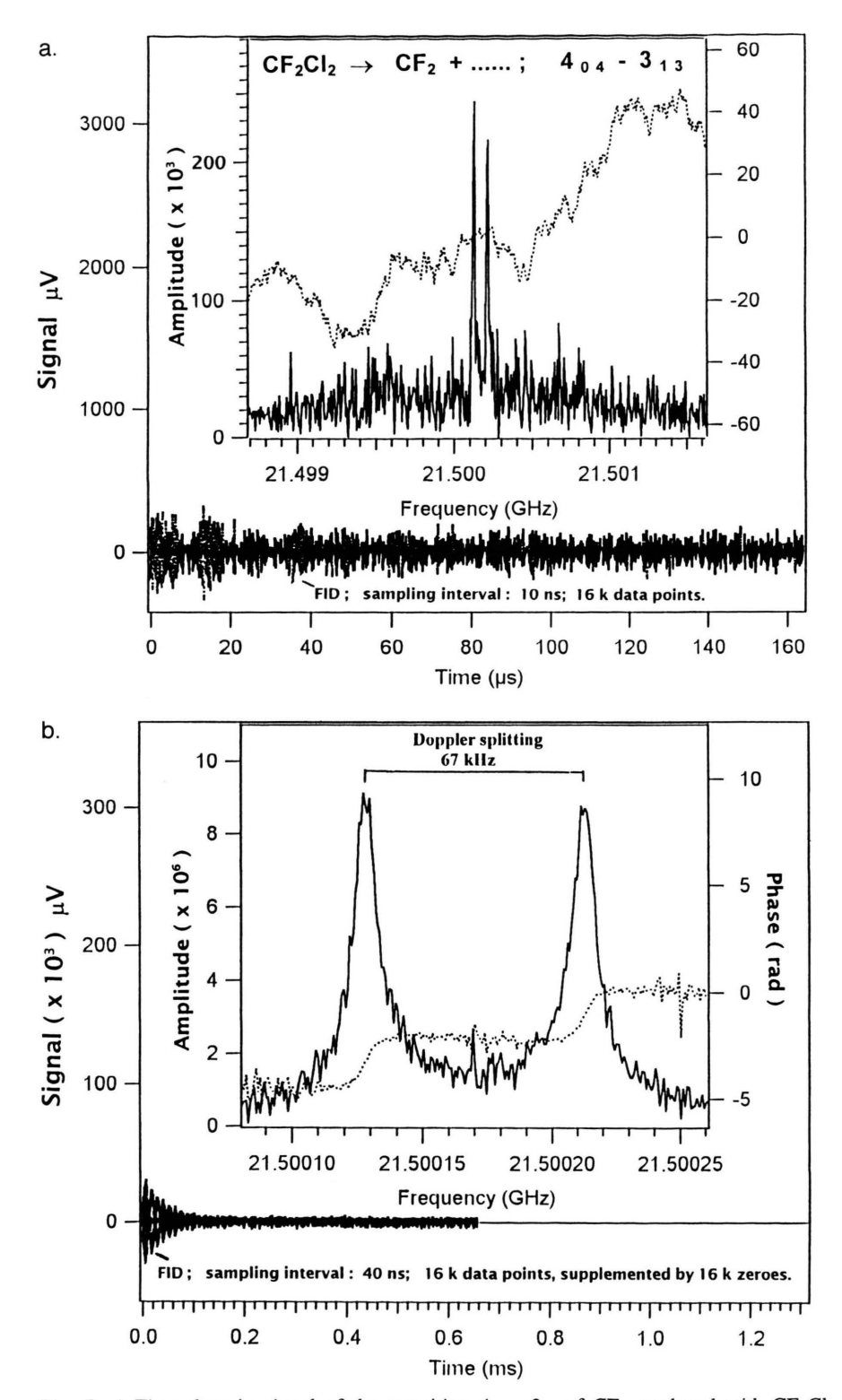


Fig. 7. a) Time domain signal of the transition 4_{04} - 3_{13} of CF_2 produced with CF_2Cl_2 . 21500.17 MHz polarisation frequency, 4 cycles. This recording demonstrates the efficiency for the production of the carbene. *Insert*: Amplitude and phase spectrum. b) Same transition recorded with 2048 cycles.

Considering that the ν_9 -mode is antisymmetric with respect to the C_{2a}-rotation around the a-axis, which exchanges the spin-(1/2) H-nuclei, the product of the rotational wavefunction (which is symmetric in the upper as well as in the lower rotational state) and the vibrational wavefunction must be antisymmetric. This requires the proton-spin function to be symmetric to give an antisymmetric overall wavefunction. Thus, at least in principle, the $1_{0.1}$ - $0_{0.0}$ rotational transition in the $\nu_0 = 1$ state should show spin rotation fine structure. However, within the resolution of the spectrometer, it does not. On the other hand, with 6.2 kHz we found its linewidth (half width at half height) about twice as large as the observed linewidth for the corresponding vibrational ground state transition. There we have observed a linewidth of 2.8 kHz under otherwise identical experimental conditions. From these data one may estimate that the average population of the first excited state within the molecular cloud is the same as would be observed in thermal equilibrium at about 350 K. Thus, within the translationally and rotationally extremely cold beam (1 - 4 K), the first excited state of the lowest bending vibration exhibits a population even in excess of its thermal value at room temperature.

b) The Difluorocarbene Radical from Dichlorodifluoro-methane

By using dichloro difluoro methane, Cl₂F₂C, supplied by Fa. Höchst, Frankfurt, as precursor in a 1% mixture with argon at a backing pressure of 1.4 bar and at discharge voltages close to 1400 V we observed difluorocarbene, CF₂. In an independent experiment CF₂ has been produced recently by Hansen [26] at our institute, who used laser photolysis combined with a MB FTMW spectrometer [27] for production and identification. CF₂ is a closed shell free radical, isoelectronic to NOF, and has been studied extensively by Kirchhoff and Lide [28], who also determined its electronic ground state potential surface from their experimental spectroscopic data. After optimization, only four measuring cycles, the FID-data taken at a sampling interval of 10 ns, were sufficient to observe the $J_{K_aK_c} = 4_{04} - 3_{13}$ b-type rotational transition with a signal to noise ratio of S/N = 9 in the Fourier transform amplitude spectrum as shown in Figure 7a. In Fig. 7b we present the Fourier transform amplitude spectrum of this transition after accumulation of 2048 FIDs with a sampling interval of 40 ns. As expected, the above transition shows no indication of further hyperfine splittings. In difluorocarbene the molecular symmetry axis coincides with the b-axis of the moment of inertia tensor. Thus, for symmetry reasons, only transitions between rotational states with K_a , K_c = even, odd \leftrightarrow odd, even do show spin rotation splitting in the vibronic ground state. In contrast, vibrational states, whose vibrational wavefuntions are antisymmetric with respect to an exchange of the F-nuclei, will show spin rotation splittings for $J_{K_aK_c}$ states with K_a , K_c = even, even and odd, odd, while transitions between states with K_a , K_c = even, odd and odd, even states cannot show spin-rotation hyperfine structure. These spin rotation splittings are currently studied by Hansen who will present his results in a forthcoming publication.

Discussion

We can state that F₂CO and H₂CCO were produced by the discharge reaction

$$H_2CCF_2 + CO_2 \rightarrow F_2CO + H_2CCO.$$
 (5)

A cycloaddition may lead to an intermediate, as indicated in (2). Unfortunately the MW spectrum of the assumed ring compound is not known. Within the discharge many other species may be produced. This may be investigated in future.

As the produced molecules presumably also occupy different vibrational excited states, it is astonishing that only the rotational transition of one of the three low energy bending states of ketene [25] could be observed.

It should be mentioned that the "discharge" method applied to acetic anhydride is for ketene much more effective. The observation of acetic acid indicates that the discharge production parallels the usual "thermal" pyrolysis, as the same molecular fractions were observed.

The observation of the radical CF₂ shows that the investigation of free radicals is a promising field for further investigations.

In general we found that the resolution of MB-FTMW spectroscopy is not remarkably reduced by the "discharge" method. Furthermore, it is a sensitive detection method of the produced molecular species.

Acknowledgement: We thank the members of the Kiel MW group and especially Prof. Dr. A. Guarnieri, Dr. U. Andresen and Dr. J. Gripp for help and discussions, Dr. J.-U. Grabow, Hannover, for help in the initial state of the project, Dipl. Chem. N. Hansen for communication of his measurements on CF₂. The mechanics

and electronics workshops gave the necessary assistance, which is greatfully acknowledged. The funds were provided by the Deutsche Forschungsgemeinschaft, the Fonds der Chemie and the Land Schleswig-Holstein.

- R. F. C. Brown, Pyrolytic Methods in Organic Chemistry, Academic Press, New York 1980.
- [2] J.-U. Grabow, W. Stahl, and H. Dreizler, Rev. Scient. Instrum. 67, 4072 - 4084 (1996).
- [3] M. D. Harmony, K. A. Beran, D. M. Angst, and K. L. Ratzlaff, Rev. Sci. Instrum. 66, 5196-5202 (1995).
- [4] J.-U. Grabow and W. Stahl, Z. Naturforsch. 45a, 1043-1044 (1990).
- [5] N. Hansen, Private communication, April 2000.
- [6] J.-U. Grabow, N. Heineking, and W. Stahl, Z. Naturforsch. 46a, 914-916 (1991).
- [7] Y. Endo, H. Konguchi, and Y. Oshima, Faraday Discuss. 97, 341-350 (1994).
- [8] M. J. Travers, W. Chen, J.-U. Grabow, M. C. Mc Carthy, and P. Thaddeus, J. Mol. Spectrosc. 192, 12-16 (1998).
- [9] U. Andresen, H. Dreizler, J.-U. Grabow, and W.Stahl, Rev. Scient. Insrum. 61, 3094-3099 (1990).
- [10] U. Andresen, H. Dreizler, U. Kretschmer, W. Stahl, and C.Thomsen, Fresenius J. Anal. Chem. 349, 272-276 (1994).
- [11] I. Merke, W. Stahl, and H.Dreizler, Z. Naturforsch. 49a, 490-496 (1994).
- [12] J.-U. Grabow, E.S. Palmer, M.C. Mc Carthy, and P. Thaddeus, to be published.
- [13] S.-R. Lin and Y.-P. Lee, J. Chem. Phys. 111, 9233-9241 (1999).
- [14] D. H. Sutter and H. Dreizler, to be published.
- [15] J. Haekel and H. Mäder, Z. Naturforsch. 43a, 203-206 (1988).

- [16] J.-U. Grabow, PhD Thesis, Kiel 1992, Chapt. IV.
- [17] J. H. Carpenter, J. Mol. Spectrosc. 50, 182-201 (1974) and citations herein.
- [18] J. H. S. Wang and S. G. Kukolich, J. Amer. Chem. Soc. 95, 4138-4141 (1973).
- [19] M. K. Lo, V. W. Weiss, and W. H. Flygare, J. Chem. Phys. 45, 2439-2449 (1966).
- [20] Amitai Halevi, Orbital Symmetry and Reaction Mechanism, Springer-Verlag, Berlin 1992, Chapt. 6.
- [21] M. J. Travers, W. Chen, J.-U. Grabow, M. C. Mc Carthy, and P. Thaddeus, L. Mol. Spectrosc. 192, 12-16 (1998).
- [22] B. Bak, D. Christensen, J. Christiansen, L. Hansen-Nygaard, and J. Rastrup-Anderson, Spectrochimica Acta 18, 1421-1429 (1962).
- [23] L. C. Krisher and L. Saegebarth, J. Chem. Phys. 54, 4553-4558 (1971).
- [24] A. P. Cox and A. S. Esbitt J. Chem. Phys. 38, 1636-1643 (1963).
- [25] R. Hinze, H. Zerbe-Foese, J. Doose, and A. Guarnieri, J. Mol. Spectrosc. 176, 133-138 (1996) and citations herein.
- [26] N. Hansen, Private communication, Jan. 2000.
- [27] N. Hansen, U. Andresen, H. Dreizler, J.-U. Grabow, H.Mäder, and F.Temps, Chem. Phys. Lett. 289, 311-318 (1998).
- [28] W. H. Kirchhoff, D. R. Lide, and F. X. Powell, J. Mol. Spectrosc. 47, 491-498 (1973).